Video Article

Potentiodynamic Corrosion Testing

Selin Munir[1], Matthew H. Pelletier[1], William R. Walsh[1]

[1]Surgical and Orthopaedics Research Laboratories, Prince of Wales Clinical School

Correspondence to: Selin Munir at selin.munir@gmail.com

URL: http://www.jove.com/video/54351
DOI: doi:10.3791/54351

Keywords: Environmental Sciences, Issue 115, Corrosion, electrodynamic, potentiostatic, polarization, topography

Date Published: 9/4/2016

Citation: Munir, S., Pelletier, M.H., Walsh, W.R. Potentiodynamic Corrosion Testing. *J. Vis. Exp.* (115), e54351, doi:10.3791/54351 (2016).

Abstract

Different metallic materials have different polarization characteristics as dictated by the open circuit potential, breakdown potential, and passivation potential of the material. The detection of these electrochemical parameters identifies the corrosion factors of a material. A reliable and well-functioning corrosion system is required to achieve this.

Corrosion of the samples was achieved via a potentiodynamic polarization technique employing a three-electrode configuration, consisting of reference, counter, and working electrodes. Prior to commencement a baseline potential is obtained. Following the stabilization of the corrosion potential (E_{corr}), the applied potential is ramped at a slow rate in the positive direction relative to the reference electrode. The working electrode was a stainless steel screw. The reference electrode was a standard Ag/AgCl. The counter electrode used was a platinum mesh. Having a reliable and well-functioning *in vitro* corrosion system to test biomaterials provides an in-expensive technique that allows for the systematic characterization of the material by determining the breakdown potential, to further understand the material's response to corrosion. The goal of the protocol is to set up and run an *in vitro* potentiodynamic corrosion system to analyze pitting corrosion for small metallic medical devices.

Video Link

The video component of this article can be found at http://www.jove.com/video/54351/

Introduction

Electrochemical techniques provide a quick and relatively inexpensive method to obtain the electrochemical properties of a material. These techniques are based predominately on the ability to detect corrosion of a metal by observing the response of the charge-transfer process to a controlled electrochemical disturbance [1-5]. Corrosion of metal implants within a body environment is critical due to the adverse implications on biocompatibility and material integrity [6]. The main factor contributing to corrosion of implants within the body is the dissolution of the surface oxide leading to an increased release of metallic ions [7-11]. This results in adverse biological reactions, which can be found locally, but with potentially systemic effects leading to the premature failure of the implant [10,12-28].

The corrosion characteristics of a test specimen are predicted from the polarization scan produced by a potentiostat. A polarization scan allows for the extrapolation of the kinetic and corrosion parameters of a metal substrate. During a scan, the oxidation or reduction of an electro-active species can be limited by charge transfer and the movement of reactants or products. These factors are all encapsulated by the polarization scan; therefore the importance of having a system that produces a reliable and repeatable polarization scan across multiple cycles is of great importance. The main focus of this manuscript is to provide a protocol identifying the rationale and steps taken to obtain a well-functioning potentiodynamic corrosion system.

Protocol

1. Construction of the Sample Holder

1. Construct the sample holder from stainless steel spacers and a M3 stainless steel threaded screw, held in place with a M3 hexagonal nut.
2. Remove the head of the threaded screw using pliers and polish the cut segment to maintain the thread pattern.
3. When all individual components are ready, assemble the electrode holders. Each electrode holder contains three spacers joined together by the M3 screws resulting in an 11.5 cm handle. Place the hexagonal nuts at the junction of the screw and spacers to lock the connection.
4. Solder (60/40% Sn/Pb) a toothless alligator clip onto the screw at the end of the rod. This will ensure a firm hold to later attach the electrode during analysis.
5. Once the electrode holders are assembled, apply multiple coats of stop-off lacquer (electrical sealant) to prevent the stainless steel rods from corroding whilst immersed in the corrosion chamber.
    1. Place all electrode holders with the samples attached to the alligator clip into a fume hood prior to coating. Place a 20 ml syringe into the fume hood. Use the syringe to collect the stop-off lacquer.

2. Turn on the fume hood and pour the stop-off lacquer into a small glass jar. Pull 10 ml of stop-off lacquer into the syringe and coat the surface of the electrode holders. Make sure not to cover the test sample, which is going to be analyzed for corrosion.
3. Coat half of each electrode holder and place in the fume hood to dry before coating the other half. This will help obtain a complete well-sealed coat without damaging the areas to be coated. Ensure that during the drying phase, the freshly coated regions do not touch other surfaces, as this will ruin the applied coat.
4. Place the electrode holders in an elevated position during drying with no contact to any surfaces. Coat the electrodes quickly due to the quick solidification of the stop-off lacquer. This completes the first layer.
5. Once dry, repeat the process to obtain 3 coats along the entire area.

6. Before commencing the corrosion run, leave the holders to dry for 24 hr after the completion of the final coat. All coating processes occur at RT, no heating or cooling steps are required although they may accelerate/decelerate the curing process.
7. **Making a faraday cage**
    1. Construct a Faraday cage by coating two plastic containers of the same size with 4 layers of aluminum foil to cover all sides.
    2. Cut two small holes out at the rim of upper plastic container to allow the electrode connection to the potentiostat and the nitrogen line to the nitrogen tank to pass through. A split design of the Faraday cage allows the upper component to be removed at the end of a run without needing to replace the lower section housing the tank.
    3. Fit the outer compartment (water chamber) into the Faraday cage. Leave the second half to the side and place on top of the lower compartment only when the corrosion vessel has been sealed (later in the procedure).

2. Cleaning of Glassware

1. Clean the corrosion vessel (700 ml cylindrical flask) before every corrosion run. Scrub the vessel with household detergent and rinse thoroughly with tap water. Repeat this step 3 times.
2. Rinse the corrosion vessel 3 times with de-ionized water (DI) water to remove potential contaminants found in tap water.
3. Once rinsing with DI water is completed pour 300 ml of 95% ethanol into the corrosion vessel and swirl around to contact all internal surfaces. Pour out the ethanol and repeat this step 3 times.
4. Leave the corrosion vessel under a fume-hood for 30 min to allow all of the ethanol to completely evaporate.
5. Take the clean, dry corrosion vessel and rinse it with the electrolyte that will be used for the corrosion run. For each rinse fill the corrosion vessel with 200 ml of the electrolyte and repeat this procedure 3 times. For this study, rinse the corrosion vessel with phosphate buffered saline (PBS). The chemical make-up of the PBS (10 L) electrolyte used throughout is 80 g NaCl, 11.5 g Na_2HPO_4, 2 g KCl and 2 g $KHPO_4$.
6. Following the rinse, fill the corrosion vessel with the required volume of PBS ready for the reaction.

3. Setup of Apparatus

1. Clamp a heater with an inbuilt circulation system to the side of the outer compartment using a clamp. The size of the outer compartment needs to be approximately 30 cm x 20 cm x 20 cm and made of either glass or polymeric to be capable of housing the smaller corrosion vessel and the heater system.
2. Fill the outer compartment with tap water until the level of water is higher than the height of the suspended electrodes within the corrosion vessel. The smaller compartment is the corrosion vessel (previously described in section 2).
3. Seal the corrosion vessel with a glass reaction lid and clamp to ensure a waterproof seal. The lid of the chamber provides six entry points for experimental and measurement apparatus.
4. Suspend a thermometer from one of the entry points of the reaction lid to provide a reading of the temperature within the corrosion cell. Suspend all three electrodes from the lid using the other 3 entry points. Use polytetrafluoroethylene (PTFE) tape to secure the seal of each connection.
5. Use a three-electrode configuration consisting of a reference, counter, and working electrode. The working electrode is the stainless steel screw (specimen under analysis). Before inserting the electrode into the corrosion vessel, wipe with an 80% ethanol soaked wipe and place in a glass beaker filled with 100 ml of PBS.
6. Use a connection pin to attach the electrode holders onto the electrode suspenders. Fit the electrode suspenders into the entry points of the corrosion vessel's lid.
7. Place the working electrode centrally with the counter and reference electrode being suspended from either side. Seal the glass entry point and the corrosion suspenders using PTFE tape.
8. For the reference electrode, use a standard Ag/AgCl. For the counter electrode, use a platinum mesh that was loosely bent to wrap around the specimen under test (working electrode).
9. Fill the Ag/AgCl electrode with 3 M KCl using a pipette. Following extensive use, change and refill the Ag Ag/Cl. To do this release the tip of the electrode to empty out the fluid into a small glass collection vessel (beaker). Once all the solution is removed insert the tip and fill with 3 M KCl.
10. Use tape on all junctions to ensure the whole chamber is sealed.
11. Once the chamber is sealed with all electrodes placed inside the corrosion vessel, set the temperature to 37 °C and open the nitrogen valve with a flow rate of 150 cm^3/min. Leave the temperature and nitrogen running for 60 min before conducting a run. Keep nitrogen running for the duration of the experiment.

4. Running Corrosion Test

1. Open the electrochemical software package, which interfaces with the USB controlled potentiostat.
2. Make electrical connections between the potentiostat and the 3 electrodes and then turn the potentiostat on.
3. Open and use the "measurement view" to view the potential and current readings of corrosion environment. During the open circuit potential (OCP) phase where no ramp potential is yet applied the current reading between the working (positive potential) and counter (negative)

electrode is around (0 ± 0.01) µA. The improper sealing of the chamber with PTFE tape can cause fluctuations in the current reading due to the chamber being aerated with nitrogen gas to remove oxygen molecules.
4. Leave the sample to equilibrate and stabilize within the corrosion vessel environment. The time duration for this varies (1 to 6 hr) and is dependent on material. Monitor the potential using measurement view to determine if stabilized conditions are reached. The potential will be constant with no fluctuations when stable conditions are reached.
5. After stable conditions are reached, start the corrosion run. However before this can be done, fill in the "corrosion program" and "cyclic voltammetry (CV)" conditions using the skeleton template provided by analytical software.
6. Select the cyclic voltammetry potentiostat procedure within the setup view from the procedure tab.
7. Enable the following parameters to be sampled for the corrosion run: the time, working electrode (WE) potential, and current for the corrosion run.
8. Select the option to automate the current range. Set the highest current in the range to be 10 mA, and the lowest current in the range to be 10 nA for the WE.
9. Ensure the final cut-off selection is controlled through the potential by setting the 'cycle back' parameter to 0.8 mV to allow the hysteresis loop to complete.
10. Record the OCP from the measurement view into the OCP parameter text box. Set the start potential 100 mV below the recorded OCP value. Set the upper vertex potential to 800 mV, the lower vertex to 100 mV below the start potential and the stop potential to 100 mV below the lower vertex potential. Set the scan rate to 0.001 V/sec and the step potential to 0.0024 V/sec. Now Press start.

5. After the Completion of the Corrosion Run

Note: After the completion of the corrosion run the polarization scan is shown within the analysis view of the software. For each polarization run the presenter view lists the OCP, the plot for E vs. t and the CV staircase which is a plot of E vs. Log (i).

1. Within each plot link, determine internal filtration of the data points, Tafel extrapolation, and plot options. Expand each link presented to show various parameters of interest, which collectively form the electrochemical parameters. The polarization scan (current density vs. potential), determines the open circuit potential, pitting potential (E_{pit}) and the protection potential (E_{pro}).
2. Tabulate the anodic and cathodic Tafel constants, the corrosion rate, the corrosion current, corrosion current density, the start potential, and end potential under the corrosion rate using the Tafel slope link.

6. Removing the Sample from the Electrode Holder

1. Prepare 3 small jars of 50 ml with dichloromethane under the fume hood.
2. Remove tested samples from the electrode holders by immersing the lower end of the holder in dichloromethane for 30 min inside a fume-hood.
3. Once detached, place the specimen into the next jar of dichloromethane and leave for 15 min. Repeat this process with the third and final rinse to get rid of any excess coating on the attachment sections of the sample.
4. Wipe the remaining sealant from the clip and sample and finally rinse with DI water.

Representative Results

At the conclusion of the procedure an *in vitro* corrosion system is setup to conduct corrosion studies. Specific procedures such as the cleaning of the corrosion vessel and the Faraday cage were introduced into the protocol to improve noise performance. The fundamental concept of a good polarization scan is to identify the electro-physical conditions of the material providing valuable information in order to understand the corrosion susceptibility of a metallic material. The procedure and protocol is critical to achieving reliable and reproducible results. Obtaining information on which optimizations can help certain problems that can occur during use, are identified and added into the current procedure. The pre-existing non-calibrated system produced a polarization scan (**Figure 1**). This scan shows a collection of scattered points, which do not directly allow the determination of the electro-physical conditions of the material under examination. The identification of the OCP was not practical and the corrosion or repassivation potentials are difficult to read. Faults found with the pre-existing setup included a polarization scan that did not reach the maximal potential and was cut off prematurely due to high noise levels. Secondly the scan during the live recording phase exhibited oscillations, which can potentially be due to instability or a high noise levels. Oscillations during the run were seen as a result of instability. Lastly consecutive scans would not deliver reproducible results making it impossible to determine the electro-physical properties of a specific material.

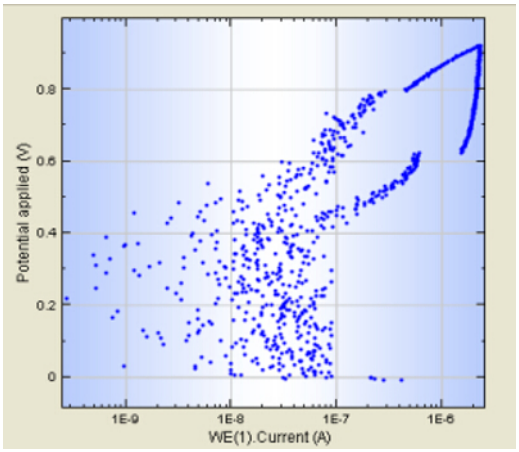

Figure 1. The polarization scan of a Nitanol sample after undergoing electrodynamic potentiostatic polarization. This figure shows a noisy plot that does not provide accurate interpretation of the corrosion parameters. Please click here to view the original version of this figure.

The improvement in noise performance is presented in (**Figure 2**). The scan shows the direction of the forward and reverse scans and specifies the point at which the protection potential (E_{pro}) and pitting potential (E_{pit}) are observed. The plot is clean with no noise or discrepancy across the whole sweep allowing the entire range to be observed cleanly. The hysteresis loop is reversed at the set potential and returns to intercept the anodic curve, identifying the protection potential. The polarization scan and Tafel plot are the outputs, which provide the fundamental parameters required. These parameters are determined from the polarization scan, therefore having a system that provides high quality scans which are reproducible and reliable is important before identifying the parameters that can be extrapolated.

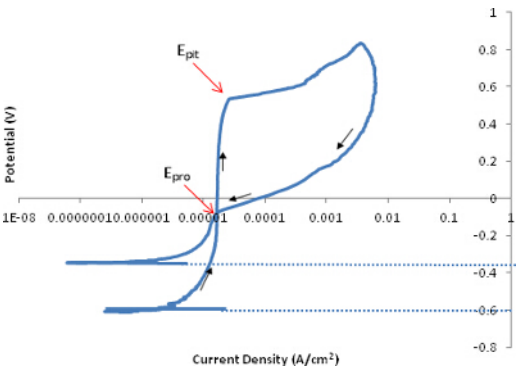

Figure 2. A polarization scan of stainless steel 316. This is a clear plot resembles a polarization scan following corrosion where the parameters of interest can be easily detected. Please click here to view the original version of this figure.

A study was conducted to analyze changes in surface topography of metal screws following pitting corrosion. The mean E_{corr} value obtained from the study was (-0.414 ± 0.05) V. The mean pitting potential for the samples was (0.49 ± 0.12) V, which was within the active region of the polarization curve. The mean protection potential of the samples was (-0.16 ± 0.02) V. Each screw formed localized pits along the surface confirming the findings from the macroscopic images showing detailed topography changes due to the formation of the pits and the changes within the pits (**Figure 3**). The quantification of the surface topography of the material shows that the roughness of the material has decreased as the overall surface roughness; of the screws R_a was (159.9 ± 7.3) µm (non-corroded) and (124.7 ± 18.3) µm (corroded). The R_a was significantly lower ($p = 0.02$) for the corroded specimen compared to the non-corroded. The average maximum height R_z being (469.3 ± 16.5) µm (non-corroded) and (683.2 ± 85.8) µm (corroded) identifies a significant difference ($p = 0.04$) for the height variation between a corroded and non-corroded sample. The mean maximum height (R_t) was lowered for non-corroded at (502.61 ± 51.2) µm in comparison to corroded screws at (592.23 ± 119.7) µm.

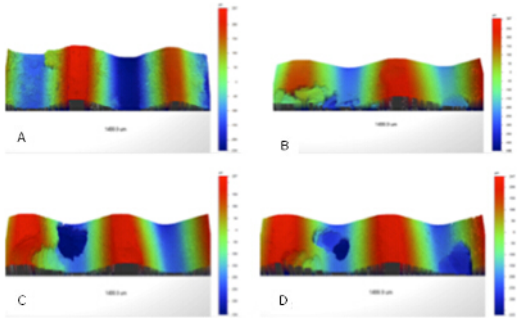

Figure 3. Images from the optical profilometer that show localized corrosion on a threaded surface. Corrosion has been detected both in the valleys and troughs of the surface. The visual observation of pitting corrosion was successfully achieved by the corrosion setup. Please click here to view the original version of this figure.

Discussion

Polarization scans produced from the stainless steel samples showed clean continuous plots correlating with scans seen in literature indicative of a well functioning corrosion system which is both reliable and reproducible [29]. Poor reproducibility of potentiodynamic pitting potentials is identified with a spread of a few hundred millivolts, with pitting potential being characterized by a stochastic process [29]. This is commonly due to the variables of temperature, halide content and potential (V); therefore the smaller variation obtained in the E_{corr} from the practical setup is indicative of the protocol and aforementioned adjustments having improved the *in vitro* setup.

A critical step in the procedure was to establish a stable environment within the reaction vessel and reduce noise. Creating and following specific steps to clean the reaction vessel prior to each run improved the results and provided reproducible and reliable readings. Contaminants within the electrolyte can alter the corrosion environment and the response of the material to corrosion, causing discrepancies in the results. Minimizing this was found to be a critical step in the protocol. The cleaning procedures in place for the electrodes and corrosion vessel remove potential impurities, which could have been a contributing factor to the discrepancies seen previously.

A second critical step within the procedure was to provide an electro shield to the sample holders to eliminate any metal contact within the chamber. The significance of shielding the metal holders completely from any electrochemical conductivity was to prevent interference of external metals. Without isolating the metal specimen under test from any other form of metal species the corrosion analysis cannot provide accurate readings of the test specimen. If the holders are not coated properly they will corrode. If corrosion is seen on metal components that are not under examination the readings cannot be used for analysis and another run would be required.

Initially the scan during the live recording phase exhibited oscillations, which can potentially be due to instability or a high noise level. Oscillations during the run were seen as result of instability. This is due to the failing of the potentiostat to maintain control of the cells potential [30]. Oscillations due to a high noise level can be from external sources, which require a degree of filtration. The key to troubleshooting was to connect ceramic disk capacitors between the electrolytes and counter electrode. Suppression capacitors are generally incorporated into alternating current line filters to suppress electromagnetic or radio frequency interference as well as reducing electrical switching noise which is commonly produced by electrical/electronic equipment. Four different magnitudes of ceramic capacitors were used to analyze their noise suppression efficacy on the polarization curve, ranging from 0.001 to 1 µF. The 0.1 µF capacitor smoothed the polarization curve significantly. All noise was suppressed; removing all spikes found in the original scans. The experimental results indicated that the inductance starts to lower the noise suppression efficacy of the 1 µF capacitor, whilst not affecting the 0.1 µF in the frequency range of the present noise.

Potentiodynamic corrosion will provide an *in vitro* corrosion testing system for materials in controlled environments. A material's corrosion capability can be assessed following any form of manipulation made to the material. The analysis of corrosion with the capability to control different parameters will provide further examination and analysis of corrosion changes in metallic materials. The proposed protocol has both limitations and benefits. The significance of this method in relation to other methods is the relatively low cost and quick process to perform a sophisticated analysis [1,4,5]. The protocol will provide a reliable source of laboratory testing to be conducted. However a limitation of the protocol is the limited number of parallel samples that can be tested at one point. The setup only provides one sample per test, which will prolong the test time for a large number of samples.

Disclosures

The authors have nothing to disclose.

Acknowledgements

The authors had no funding provided for this study.

References

1. Isaacs, H. S. Aspects of corrosion from the ECS Publications. *J. Electrochem. Soc.* **149** (12), 85-87 (2002).
2. Fontana, M.G., Greene, N.D. *Corrosion Engineering.* 2nd edn, McGraw-Hill, NY, USA, (1978).

3. Pourbaix, M. Electrochemical corrosion of metallic biomaterials. *Biomaterials.* **5** (3), 122-134 (1984).
4. Rechnitz, G. A. in *Controlled-Potential Analysis.* Pergamon Press Inc, New York, (1963).
5. Silverman, D. C. in *Uhlig's Corrosion Handbook.* (ed R W Revie) Ch. 68 John Wiley and Sons Inc, (2000).
6. Gurappa, I. Characterization of different materials for corrosion resistance under simulated body fluid conditions. *Mater Charact.* **49** (1), 73-79 (2002).
7. Antoniou, J. *et al.* Metal ion levels in the blood of patients after hip resurfacing: a comparison between twenty-eight and thirty-six-millimeter-head metal-on-metal prostheses. *J Bone Joint Surg Am.* **90 Suppl 3** 142-148 (2008).
8. Billi, F., & Campbell, P. Nanotoxicology of metal wear particles in total joint arthroplasty: a review of current concepts. *J Appl Biomater Funct Mater.* **8** (1), 1-6 (2010).
9. Bradberry, S. M., Wilkinson, J. M., & Ferner, R. E. Systemic toxicity related to metal hip prostheses. *Clin Toxicol (Phila).* **52** (8), 837-847 (2014).
10. Davda, K., Lali, F. V., Sampson, B., Skinner, J. A., & Hart, A. J. An analysis of metal ion levels in the joint fluid of symptomatic patients with metal-on-metal hip replacements. *J Bone Joint Surg Br.* **93** (6), 738-745 (2011).
11. Clarke,M.T., Lee, P.T., Arora, A., Villar, R.N. Levels of metal ions after small and large diameter metal-on-metal hip arthroplasty. *J Bone Joint Surg Br.* **85** (6), 913-917 (2003).
12. Brown, S. A., Hughes, P. J., & Merritt, K. *In vitro* studies of fretting corrosion of orthopaedic materials. *J Orthop Res.* **6** (4), 572-579 (1988).
13. Bryant, M. *et al.* Characterisation of the surface topography, tomography and chemistry of fretting corrosion product found on retrieved polished femoral stems. *J Mech Behav Biomed Mater.* **32** 321-334 (2014).
14. Jantzen, C., Jørgensen, H. L., Duus, B. R., Sporring, S. L., Lauritzen, J. B. Chromium and cobalt ion concentrations in blood and serum following various types of metal-on-metal hip arthroplasties. A literature review. *Acta Orthopaedica.* **84** (3), 229-236 (2013).
15. Campbell, P. *et al.* Histological Features of Pseudotumor-like Tissues From Metal-on-Metal Hips. *Clin. Orthop. Relat. Res.* **468** (9), 2321-2327 (2010).
16. Cook, S. D. *et al.* The *in vivo* performance of 250 internal fixation devices: a follow-up study. *Biomaterials.* **8** (3), 177-184 (1987).
17. Cooper, H. J., Urban, R. M., Wixson, R. L., Meneghini, R. M., & Jacobs, J. J. Adverse local tissue reaction arising from corrosion at the femoral neck-body junction in a dual-taper stem with a cobalt-chromium modular neck. *J Bone Joint Surg Am.* **95** (10), 865-872 (2013).
18. Langton, D.J., Sprowson, A.P., Joyce, T.J., Reed, M., Carluke, I., Partington, P., Nargol, A.V. Blood metal ion concentrations after hip resurfacing arthroplasty. *J Bone Joint Surg Br.* **91** (10), 1287-1295 (2009).
19. Langton, D.J., Jameson, S.S., Joyce, T.J., Webb, J., Nargol, A.V. The effect of component size and orientation on the concentrations of metal ions after resurfacing arthroplasty of the hip. *J Bone Joint Surg Br.* **90-B** (9), 1143-1151 (2008).
20. Daniel, J., Ziaee, H., Pradhan, C., & McMinn, D. J. Six-year results of a prospective study of metal ion levels in young patients with metal-on-metal hip resurfacings. *J Bone Joint Surg Br.* **91** (2), 176-179 (2009).
21. De Haan, R. *et al.* Correlation between inclination of the acetabular component and metal ion levels in metal-on-metal hip resurfacing replacement. *J Bone Joint Surg Br.* **90** (10), 1291-1297 (2008).
22. Dijkman, M. A., de Vries, I., Mulder-Spijkerboer, H., & Meulenbelt, J. Cobalt poisoning due to metal-on-metal hip implants. *Ned Tijdschr Geneeskd.* **156** (42), A4983 23075776 (2012).
23. Fisher, J. Bioengineering reasons for the failure of metal-on-metal hip prostheses: an engineer's perspective. *J Bone Joint Surg Br.* **93** (8), 1001-1004 (2011).
24. Goldberg, J. R. *et al.* A Multicenter Retrieval Study of the Taper Interfaces of Modular Hip Prostheses. *Clin. Orthop. Relat. Res.* **401** (401), 149-161 (2002).
25. Ingham, E., & Fisher, J. Biological reactions to wear debris in total joint replacement. *Proc Inst Mech Eng H.* **214** (1), 21-37 (2000).
26. Gilbert, J.L., Buckley, C.A., Jacobs, J.J. *In vivo* corrosion of modular hip prosthesis components in mixed and similar metal combinations. The effect of crevice, stress, motion and allot coupling. *J. Biomed. Mater. Res.* **76** (1), 1533-1544 (1993).
27. Browne, J.A., Bechtold, C.D., Berry, D.J., Hanssen, A.D., Lewallen, D.G. Failed metal-on-metal hip arthroplasties: a spectrum of clinical presentations and operative findings. *Clin. Orthop. Relat. Res.* **468** (9), 2313-2320 (2010).
28. Jantzen, C., Jorgensen, H. L., Duus, B. R., Sporring, S. L., & Lauritzen, J. B. Chromium and cobalt ion concentrations in blood and serum following various types of metal-on-metal hip arthroplasties: a literature overview. *Acta Orthop.* **84** (3), 229-236 (2013).
29. Frangini, S., De Cristofaro, N. Analysis of galvanostatic polarisation method for determining reliable pitting potentials on stainless steels in crevice-free conditions. *Corros Sci.* **45** (12), 2769-2786 (2002).
30. Bio-Logic. *Potentiostat stability mystery explained. Application Note 4.* 1-7, http://www.bio-logic.info/assets/app%20notes/Application%20note%204.pdf (2015).

